SYSTEMS FOR FAST ACTUATED DROOP NOSES AND FLAP-TABS FOR DYNAMIC LOAD CONTROL

K. Krall*, L.-H. Lemke*, F. Thielecke*, J. Müller**, C. Breitenstein***
* Hamburg University of Technology, Institute of Aircraft Systems Engineering, Nesspriel 5, 21129 Hamburg, Germany
** University of Stuttgart, Institute of Aerodynamics and Gas Dynamics, Pfaffenwaldring 21, 70569 Stuttgart, Germany
*** University of Braunschweig - Institute of Technology, Institute of Fluid Mechanics, Hermann-Blenk-Str. 37, 38108 Braunschweig, Germany

Abstract

Dynamic load control offers a high potential for the improvement of aerodynamic performance and increase in passenger comfort. However, it is unclear if the implementation is feasible or even possible regarding the actuation system design. The demand of actively reducing gust loads acting on the wing results in challenging requirements for the actuation systems regarding high actuation speeds and loads. In this paper, promising actuation concepts for fast actuated droop noses and flap-tabs will be analysed based on preliminary designs. Furthermore, the impact on the overall system level is discussed.

Keywords

Droop nose, dynamic load control, fast actuation, preliminary sizing, systems architecture, system design

1. INTRODUCTION

Flight control devices used on wings of commercial aircrafts are predominantly used for either steering the aircraft by inducing rolling, pitching or yawing manoeuvres or for high-lift capabilities by providing lift augmentation in low airspeed operations. Conventional flight control devices thus largely fulfil one function only. However, a demand for new functions of flight control systems arises. One of these new required functions is active dynamic load control, which reduces increased loads on the wing, occurring as a result of gusts or manoeuvres, by adequate reactions of the control surfaces. Ullah et al. [1] show that the use of trailing edge flap-tabs and droop nose devices (DN) for load control can reduce the gust-induced bending moment and torsional loads on the wing structure. According to [1] the flap-tabs reduce the gust-induced wing bending moment while increasing the torsional loads. To counter the torsional load increase, DN on the leading edge are utilised.
Due to the requirement of reactive reduction of gust loads, high actuation speeds and actuation loads result during cruise flight. Furthermore, the development of thinner wing profiles creates an additional challenge to implement high-performance actuation systems in the confined installation space. Preliminary system designs and models are needed to investigate feasibility on a system level for fast actuated DN and flap-tabs used for dynamic load control. Within the scope of the study, the consequences resulting from the implementation of rapidly actuated control surfaces are analysed on the overall system level. The aim is to detect limits and set recommended actions for the use of a dynamic load control system. For this, the requirements and conditions are defined in section 2. In section 3 the system architecture for the actuation system is discussed to give a basis for the preliminary actuation system design in section 4. Based on the results, simulation models are introduced and used for performance analysis in section 5. The effects of the overall system level are finally given in section 6.

2. REQUIREMENTS AND CONDITIONS

The DLR LEISA configuration [2; 3], which represents a short to medium range, single aisle twin engine aircraft, is used as the reference configuration for this paper. The control surfaces investigated in this paper are based on the multifunctional control surfaces developed in the Pro-HMS project [2]. A schematical depiction of the adapted control surfaces of the LEISA wing is given in figure 1.

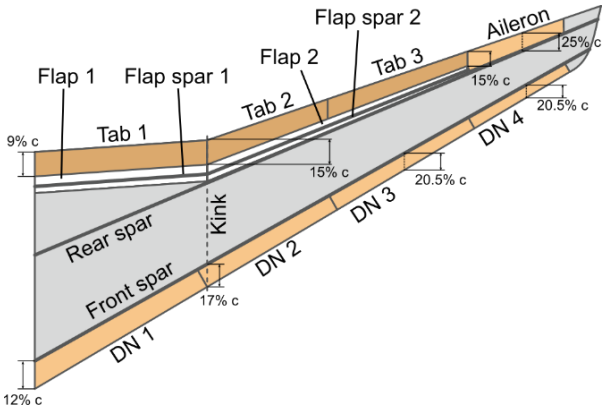

FIGURE 1. Schematic representation of control surfaces on the LEISA wing

The control surfaces investigated in this paper consist of DN on the wing leading edge and flap-tabs as well as ailerons on the trailing edge. The high-lift capabilities of this configuration are not discussed in this paper and only load

alleviation functions during cruise are investigated. Thus, only the DN, tabs and the aileron are analysed, since the flaps are not required for this purpose. According to the wing profile and the spar position, the installation space for the actuation systems can be acquired.
Based on aerodynamic CFD calculations for gust and manoeuvre scenarios, carried out at the Institute of Aerodynamics and Gas Dynamics (IAG) of University of Stuttgart, regarding the gust loads, and the Institute of Fluid Mechanics of TU Braunschweig, regarding manoeuvre loads, a critical design scenario could be identified. The here used method differs from the work of Ullah et al. [1], by utilizing a Fluid-Structure Coupling, accounting for the wing elasticity, as presented in [4]. Additionally, a redesigned version of the LEISA aircraft to Ullah et al. is investigated, see [4]. This results in a different cruise condition at Ma=0.8 and h=10500m used within this work. The scenario is represented by the design-critical vertical "1-cos"-type gust event with a wavelength of 50 m and design gust velocity of 14.5 m/s, based on CS-25.341 [5] and Ullah et al. [1], that requires active lift redistribution by the DN and tabs. The active lift adaptation leads to an ambitious reduction of the wing bending moment of 88% and 31% reduction of the wing torsional moment. The definition of bending and torsional moment used here is given in [4]. The resulting torques, actuation speeds and maximum deflections required at the hinge position of the individual control surfaces are given in table 1 for DN (leading edge) and table 2 for tabs and aileron (trailing edge).

	DN 1	DN 2	DN 3	DN 4
M [Nm]	13702	8991	4819	2533
$\dot{\eta}$ [°/s]	149	232	177	40
η_{max} [°]	-16.7	-15.6	-11.9	-2.7

TAB 1. Critical design case for DN due to gust

	Tab 1	Tab 2	Tab 3	Aileron
M [Nm]	2251	2740	1165	1782
$\dot{\eta}$ [°/s]	107	124	136	136
η_{max} [°]	-7.2	-8.3	-9.1	-6.2

TAB 2. Critical design case for tabs and aileron due to gust

Regarding system safety analysis, the required reliability of the load alleviation system has to be determined. According to EASA regulations CS-25 K25.2 [5], the factor of safety considered to design the structure can be reduced, if systems influencing the structural behaviour show high enough reliability. Since the fast actuated DN and flap-tabs represent a dynamic load control system acting on the structure by reducing critical loads, the reliability of the system has to be investigated. The load alleviation function is assumed to only fail, if the function of three tabs or three DN is lost. The loss of any single tab or DN is thus less critical, but is still conservatively assumed to be smaller than $10^{-4}\ 1/f_h$. To ensure roll capabilities as well as flutter suppression, the probability of loss of control of one aileron is assumed to be $10^{-7}\ 1/f_h$. The flaps of the configuration will be actuated by a conventional actuation system consisting of a continuous shaft with central drive. The tabs located at the trailing edge of the flaps as well as the DN have to be actuated individually to ensure optimal control of the wing shape.

3. ACTUATION SYSTEM ARCHITECTURE

As the tab actuation systems are positioned inside the flaps, the movement of the flaps during start and approach has to be taken into account when designing the power and signal supply. In case a hydraulic power supply is used, twists of the supply line have to be prevented by a guide concept or telescopic solution. Furthermore, the hydraulic supply line may lie outside the wing geometry, if the flap is extended. This poses a risk of damage, especially during landing. A damaged supply line could easily be excluded from the network using a valve, but hydraulic fluid would escape for a short time. For the use of an electrical power supply, there is a risk of damaging the supply cables during landing operations as well. Compared to the hydraulic power supply however, possible damage to the cables is less critical, since no fluid is lost from the aircraft and the faulty cable can be disconnected from the network. Even so, additional mechanical stress would be applied on the cables during operation of the flaps, which is why it must be ensured that the cables are loaded as little as possible. An exemplary cable routing using a cable chain guided along the flap kinematic is depicted schematically in figure 2. With concepts like this the mechanical stress on the cables can be minimized.

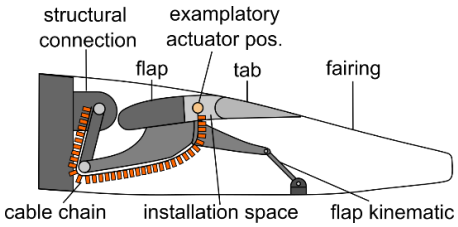

FIGURE 2. Schematic representation of cable routing for tab actuation using a cable chain

Based on the risk, potential damage on hydraulic supply lines poses, as well as the general trend of electrification of aircraft systems, an electrical power and signal supply is selected for the tab actuators. To further study the effect of a more electric aircraft, the supply for the DN and ailerons is determined to be electrical as well. Since all devices have to be actuated individually, the selection of possible drive architecture concepts is reduced to a single surface drive and station drive. The mentioned concepts are exemplary shown in figure 3.

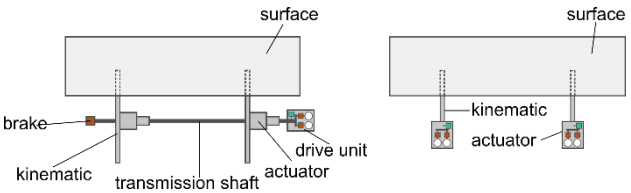

FIGURE 3. Exemplary implementation of a single surface drive (left) and station drive (right)

Compared to the station drive, there is an increased inertia in the single surface drive concept due to additional components, such as the transmission shaft and gears. The

requirement for very high actuation speeds imposes the need for minimum system inertia. Furthermore, an active-active operated station drive allows the load to be distributed over two drive systems, reducing the components dimensions and thus increasing the chances of meeting the restrictive installation space requirements. It is assumed that force conflict between the actuators is avoided through control concepts. Possible different compensation methods are given in [6]. For these reasons, an active-active station drive architecture will be further investigated in this paper.

3.1. Considered Kinematics

The tabs and DN are required to perform high velocity rotary movement about the respective hinge line. On the basis of minimal weight, complexity, required installation space and actuation load, a selection of three possible kinematics depicted in figure 4 has been compiled. The lever kinematic (LK), conventionally used for ailerons, consists of a lever attached to the device, which is connected to a linear actuator. Thus, transferring the translatory movement of the actuator into a rotatory movement of the device. Similarly, the four-bar linkage (FBL) consists of a lever positioned on the device. This lever is coupled to a rod, which in turn is connected to the motor lever, forming a four-bar linkage. This kinematic can thus reduce the required torque on the motor depending on the lever ratios and enables free positioning of the motor. The simplest kinematic solution is to position a hinge line motor (HLM) on the hinge line to directly operate the device.

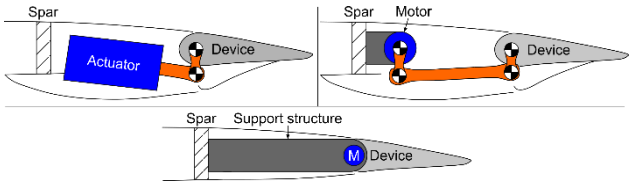

FIGURE 4. Schematic representations of considered kinematic concepts. Upper left: Lever Kinematic (LK), Upper right: Four-Bar Linkage (FBL), Lower: Hinge Line Motor (HLM)

3.2. Considered Actuation Systems

Electrohydraulic actuators (EHA), electromechanical actuators (EMA) and rotational electromechanical actuators (RotEMA) are considered as possible actuators. A depiction of this selection is given in figure 5.

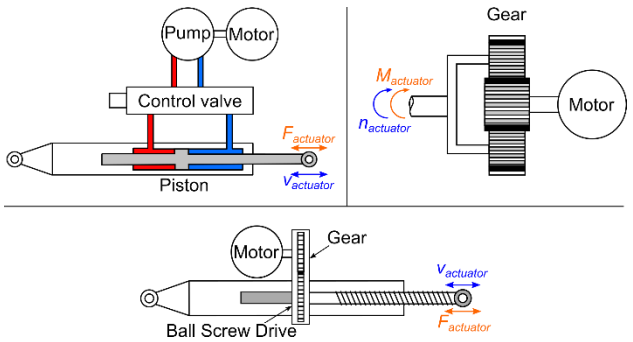

FIGURE 5. Schematic representations of considered actuator concepts. Upper left: EHA, Upper right: RotEMA, Lower: EMA

The EHA consists of a local hydraulic pump driven by an electric motor, which actuates a piston via a control valve. The concept of an EMA consists of an electric motor, which drives a ball screw via a transmission gear. The ball screw translates the rotational movement into linear motion. Similarly, the RotEMA represents an electric motor connected to a gear box. The RotEMA thus represents the only actuation system producing rotational motion as output. Assumptions regarding the actuation systems relevant for preliminary design are given in section 4.

3.3. Reliability Analysis

Based on the selected station drive concept, a reliability analysis is carried out to confirm whether the requirements set out in section 2 regarding failure probabilities can be met using different actuator concepts. For this purpose, a Common Cause Analysis (CCA) based on the SAE guideline ARP 4761 [7] is conducted and the failure probability of a potential actuation system is estimated.
As part of the CCA a Common Mode Analysis (CMA) must be conducted taking failures of several components or systems that occur as a result of a single cause into account. When applying CMA to the chosen station drive architecture, it is important to use redundant signal and supply systems ensuring all devices to be operable in the event of a single failure. Furthermore, it is assumed that simultaneous failure of soft- and hardware caused by the same malfunction is prevented by dissimilar manufacturing and coding.
Regarding Zonal Safety Analysis (ZSA) it is investigated whether parts of the system are positioned in close proximity to each other, so that damage at this zone would cause simultaneous failure of several components. The advantage of the station drive architecture is the spatial mechanical separation of the actuator stations. There is however a dependency in the routing of the power and signal supply. A particularly critical source of damage is represented by the rotor burst, in which a turbine blade detaches and damages the structure [8]. The critical zone affected by such a rotor burst lies between engine and fuselage, as shown simplified in figure 6.
The routing given in figure 6 ensures all networks supply the same number of actuators and as few devices as possible fail in the event of zonal damage. Using the routing given in figure 6, only the inner droop nose would fail due to a rotor burst. Each actuator is equipped with a redundant signal and power supply. The number of four signal and power supply networks does not necessarily correspond to the number of generators or computers needed.
The final part of the CCA to be conducted is the Particular Risk Analysis (PRA), considering disturbances that occur outside the system boundary and can lead to simultaneous failure of several subsystems. Relevant causes of failure are fire, non-containment of high energy devices such as engines, high pressure air duct rupture, leaking fluids, hail, ice, snow, bird strike and lightning strike. It is assumed that all relevant causes of failure are accounted for by conventionally used prevention methods such as using low-flammability hydraulic fluids, routing accounting for rotor burst, structural protection from precipitation and leaks and electrical shielding of the components.

©2024

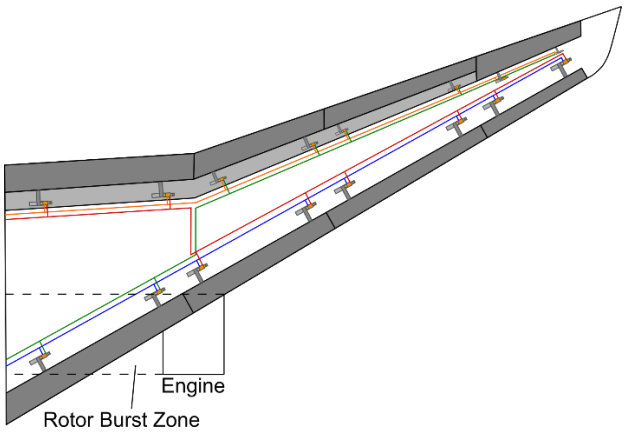

FIGURE 6. Signal and supply routing with depicted rotor burst zone

Reliability Block Diagrams (RBD) are used to estimate the failure probabilities of the chosen actuation system EHA and EMA. For RotEMA the same RBD used for EMA is utilised. The RBD diagrams, representing the system architectures and component failure probabilities based on [9;10;11], are given in figure 7. For the electrical power supply and the signal supply by the computers, the redundant design resulting from the CCA is used. The remote electronic units (REU) are redundantly implemented as well to reduce the overall probability of failure. The motor control electronic (MCE), the motor and the EHA or EMA, respectively, are singular in the RBD as only one actuator station is considered.

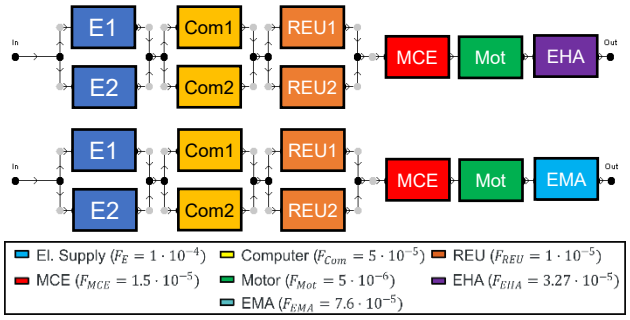

FIGURE 7. RBD of one EHA and EMA in a station drive architecture

Based on the RBD, the probability of failure for the EHA system architecture is $5.27 \cdot 10^{-5}\ 1/f_h$ and for the EMA or RotEMA system architecture it is $9.6 \cdot 10^{-5} 1/f_h$. Thus, the reliability requirements of $10^{-4}\ 1/f_h$ given in section 2 for DN and tab actuation systems are already fulfilled by a simplex actuation, provided failure cases are detected by a sensor system. Regarding the actuation of the aileron, a duplex actuation architecture is required.
The available installation space is very limited. To minimize the actuation loads of a single actuator and subsequently reducing component dimensions an active-active duplex actuation architecture is chosen for all devices.

4. PRELIMINARY ACTUATION SYSTEM DESIGN

A tool created at the Institute of Aircraft Systems Engineering of the Hamburg University of Technology is used to preliminary design and optimize kinematics and actuators based on loads, actuation speeds and available installation space. A genetic optimisation algorithm NSGA-II (Non-Dominated Sorting Genetic Algorithm II) was used for this purpose, the process of which is shown in figure 8. A full description of the algorithm is given in [12].

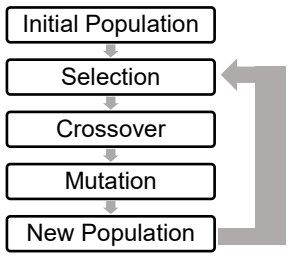

FIGURE 8. Schematic process of the genetic algorithm

First, a population of individuals is created and randomly initialized. An individual represents a possible vector of input values used for the design. The design, which is presented in more detail below, is carried out on the basis of the individuals' input values and the results are rated using an evaluation function. The following steps are iteratively run through until a termination criterion, which is defined as either reaching a maximum number of generations or achieving a certain rating, is met. A selection procedure is used to select two individuals for recombination. The selection is random, but well-scored individuals have a higher probability of being selected. Based on the input values of the selected individuals, new individuals are created by crossover and mutation of the parameters, which are used for the next design generation, thus closing the loop [13]. The variables to be optimized are power, difference between maximum and minimum actuator load for different load cases, installation space and mass. All optimization variables are to be minimized.
While loads, velocities, strokes and position data are derived from the movement of the kinematic components, the rods are designed for bending, torsion and tension to determine necessary diameters and masses. With the help of design routines, based on [6;14] and various industry catalogues, mass, power and geometrical dimensions of the actuator concepts can be generated. Furthermore, a simplified support structure for the actuator based on the weight of the designed actuation system is calculated.
Regarding the preliminary design of the EHA, the hydraulic pressure is assumed to be $p_{hyd} = 207\ bar$, representing conventional aviation standards [15]. The use of higher pressures could reduce the actuator dimensions but standard values were used for better comparability. Component efficiencies are assumed to be $\eta_{Pump} = 90\%$ for the pump, $\eta_{Motor} = 95\%$ for the motor and $\eta_{mech,hyd} = 80\%$, accounting for various mechanical and hydraulic losses. For optimal utilization of installation space, all components of the EHA except for the piston are placed lengthwise parallel to the spar. Since the component lengths represent the largest dimension, installation space can be saved this way.
For EMA and RotEMA, the following assumptions are made. The transmission gear is designed as a planetary gear representing a compromise between gearbox diameter and transmission rate. A motor efficiency of $\eta_{Motor} = 95\%$ and general gear efficiency for transmission gear and ball screw drive of $\eta_{gear} = 95\%$ is assumed. For the design of the bearings, a service life of $L_h = 60000\ h$ is chosen. Preliminary analysis has shown that electric

©2024

motors, which scale in diameter according to the required torque, will not fulfil the installation space requirements. By connecting several electric motors in series, the applied torque per motor can be reduced thus reducing the individual motor diameter. The diameter of the actuation system is therefore driven by the gearbox, which also scales via the torque. The number of motors to be used is chosen so that the diameter of the motors is smaller the gearbox.

4.1. Preliminary Actuation System Design Results

Through the optimisation method detailed in section 4, results for the given kinematics and actuators with regard to the required performance and masses for the tabs, DN and ailerons were generated. In table 3, table 4 and figure 9, the results of the preliminary actuation system design for both wing sides are depicted. It is evident that a very high power demand and severe masses result from the optimization, particularly for the actuation system of the DN. The power needed to only actuate the leading edge devices already exceeds the typical electric power generated by Airbus A320-like engines of ca. 200 kW [16]. Investigation of the impact of the actuation system mass on the total aircraft mass is done in section 6. Lastly, the challenging installation space requirements become evident in figure 9. For EHA and EMA, combined with the lever kinematic, fairings on the lower wing side will be needed for tab 2 and 3 and the front spar will be penetrated by the DN actuation system. If a RotEMA is used with a four-bar linkage, the installation space requirements for the trailing edge devices are fulfilled, but the front spar is penetrated. The use of a hinge line RotEMA results in the need for upper wing side fairings on the tabs 2 and 3 as well as the aileron and penetration of the front spar at DN 2 to 4.

	LK + EHA	LK + EMA	FBL + RotEMA	HLM + RotEMA
System mass [kg]	194	93	163	205
System power [kW]	51	36	41	36

TAB 3. Optimization results of combinations of different kinematics and actuators for the tabs and ailerons

	LK + EHA	LK + EMA	FBL + RotEMA	HLM + RotEMA
System mass [kg]	885	153	467	643
System power [kW]	365	250	251	250

TAB 4. Optimization results of combinations of different kinematics and actuators for DN

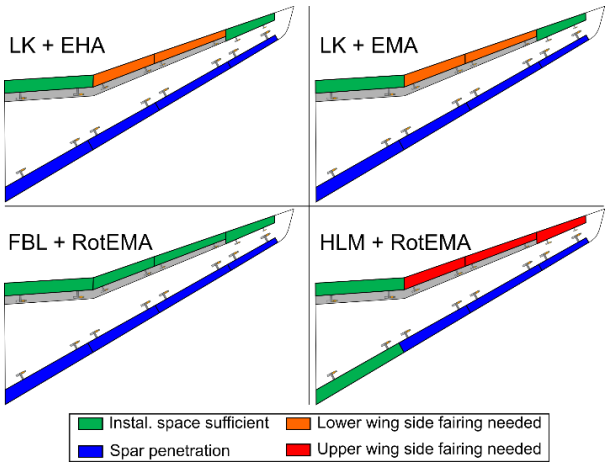

FIGURE 9. Fulfilment of installation space requirements for combinations of kinematics and actuators

The sizing laws used for the actuators are verified for actuation speeds for conventional flight control devices. The requirements given in table 1 and 2 far exceed typical actuation speeds [17]. Thus, the results given in table 3 and 4 are based on extrapolation. Which is why the actuation system mass for the DN varies strong between the different actuation concepts. The further works in this paper will focus on the four-bar linkage with RotEMA, since this concept does not require any fairings and yields comparatively moderate mass and power demands.

4.2. Impact of reduced actuation speed

The results display that the proposed high load reduction is not feasible with the assumed available power and current actuator technology used in the aerospace industry, considering the system level impact. In order to achieve a compromise between load alleviation requirements and systems feasibility, the following actions can be made:

- Reduction of deflection and thus reducing actuation speed,
- Changing the device segmentation, for example by bisecting the devices,
- Changing the device size,
- Moving the spar placement or changing the spar geometry,
- Positioning the actuation systems inside the devices.

In this paper, the impact of reduced device deflection and thus actuation speed shall be further investigated for the combination of the four-bar linkage with RotEMA. According to [16], ca. 200 kW of electric power is generated by the engines of A320-like aircrafts. To account for other electric devices and losses, it is assumed that 60 kW of electric power can be utilized for dynamic load control in cruise conditions per wing, yielding 120 kW for both wing-sides. According to [1], the flap-tabs reduce the gust-induced wing bending moment while increasing the wing torsional loads and the DN are used to compensate these additional torsional loads. The torsional cross-section of the wing inside the kink is relatively large and additional reinforcements are implemented due to the high loads induced by the engine and the landing gear. Thus, it is assumed, that additional torsional loads can be compensated in this area by the structural reinforcement itself and lower compensation by the DN is needed. Based on these assumptions, an architecture with reduced and

©2024

reallocated power demand is proposed in figure 10 and table 5.

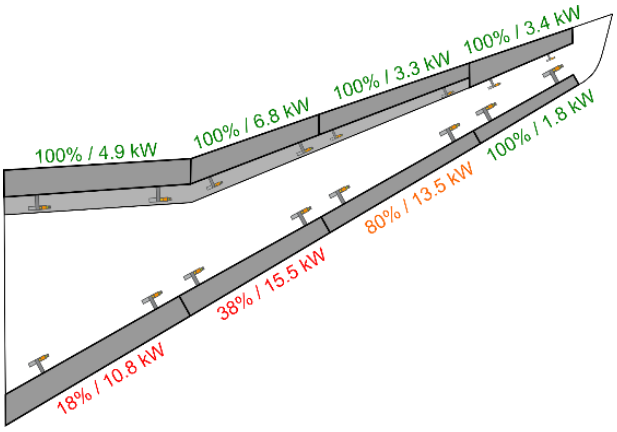

FIGURE 10. Reduced and reallocated power demand for load control devices

	FBL + RotEMA
System mass [kg]	262
System power [kW]	120

TAB 5. Optimization results for chosen kinematic and actuator with reduced actuation speed

The reduction of actuation rates of DN 1 to 3 were done arbitrarily, to reduce the total power needed for load control to 120 kW. However, due to previously mentioned assumed reinforcements close to the fuselage, compensating additional torsional loads, preserving the actuation speed for the outer DN was prioritised. In future works the impact of reduced deflections of DN should be further discussed, especially regarding aerodynamic and structural consequences.

5. SIMULATION MODELS AND PERFORMANCE ANALYSIS

Simulation models are used to verify the results of the preliminary design and to show dynamic behaviour, based on the given scenarios, accounting for previously unconsidered aspects such as inertia. The multi-body models (MBM) were created in *Matlab Simulink/Simscape* and represent rigid components of the four-bar linkage, selected in section 4.1, and the respective devices. A rigid modelling is considered sufficient, since flexible deformation of the components is assumed to be neglectable. The actuator models for the RotEMA, also selected in section 4.1, were created in *Matlab Simulink/Simscape* as well.
The system boundary is chosen so that only the actuator and the respective flap are represented in the model. As a simplification, it is assumed that both the power supply and the signal supply originating from the flight controller are transmitted to the actuators without errors, noise, latency, fluctuation or any other interference. Likewise, no fault cases are considered. The power supply and the control signals represent the inputs for the models. The MBM four-bar linkage consists of rod elements connected via joints. The lengths and diameters result from the preliminary design, presented in section 4.1, while the component inertia is determined by the MBM. The computed component masses of the MBM verify the preliminary determined masses. The models of the devices were generated based on the aircraft geometry assuming a wing wall thickness of 3 mm. For a more comprehensible representation and to visualize component dimensions, the installation space is shown as well. When visualizing the MBM of the flap-tabs, the geometry of the entire flap is not shown and only the spar of the flap is depicted, indicating the available installation space. An exemplary representation of the MBM for DN 1 and tab 1 in neutral as well as deflected position is shown in figure 11, where the kinematic components are depicted red, the actuators are depicted as a dark grey cube and the relevant spar is depicted as a grey beam.

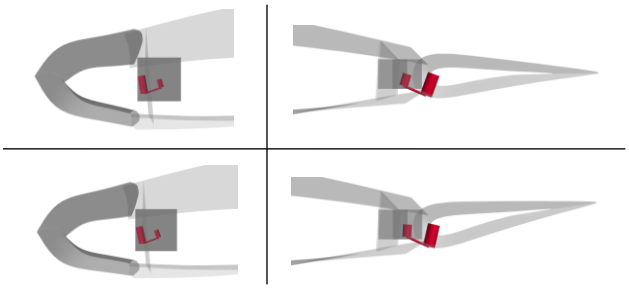

FIGURE 11. MBM for DN 1 (left) and tab 1 (right), in neutral (upper) and deflected (lower) position

The commanded motor angle acts as an input signal and is passed to the motor control unit, which is modelled as a PI-controller and modulates the electrical supply to the permanent magnet synchronous motor (PMSM). The PMSM, which is based on [6], is connected to a simple gear box model, whose output is connected to the kinematic. The actuator model is shown in figure 12. The load data is introduced as point loads at the actuator positions, assuming an even load division between the actuator stations due to symmetric positioning. In order to reduce transient effects, the load is continuously increased within the first five seconds and the neutral device position is held until the gust load is introduced at 20.1 s, followed by a commanded deflection of the devices.

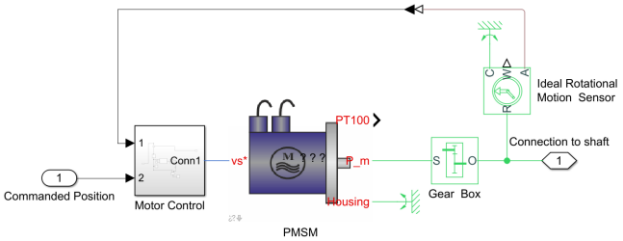

FIGURE 12. Simulation model of the RotEMA

The motor angle, device angle and one motor's power consumption, based on the reduced requirements given in section 4.2, are depicted exemplary in figure 13 for DN 1 and figure 14 for tab 1, for the relevant time the gust interacts with the wing. Figure 13 and 14 indicate the reference signal is followed very well and both the maximum actuation speed and the required deflection angle of 3° for DN 1 (18% of initial maximum deflection) and 7.2° for tab 1, can be achieved. Due to inertia, which was not accounted for in preliminary design, the motor angle

lags slightly behind the reference signal. The power demand of the simulated motor models verifies the preliminary results. It is assumed that both motors per device generate the same power demand, thus a total maximum power demand for actuation of DN 1 of 11.4 kW and for tab 1 5.5 kW arises, resulting in a deviation of preliminary design power demands of 5% for DN 1 and 12% for tab 1 which shall suffice to verify the order of magnitude. Lastly, it shall be examined if the designed actuation system is oversized. For this an exemplary 50% higher deflection angle and thus 50% higher actuation rate is commanded in the simulation for tab 1, as depicted in figure 15. As seen in figure 15, the deviation between the reference signal and motor angle differs greatly, indicating the motor to be undersized for actuation speeds of 150%. This verifies the motor is not oversized for the actuation speeds given in table 2.

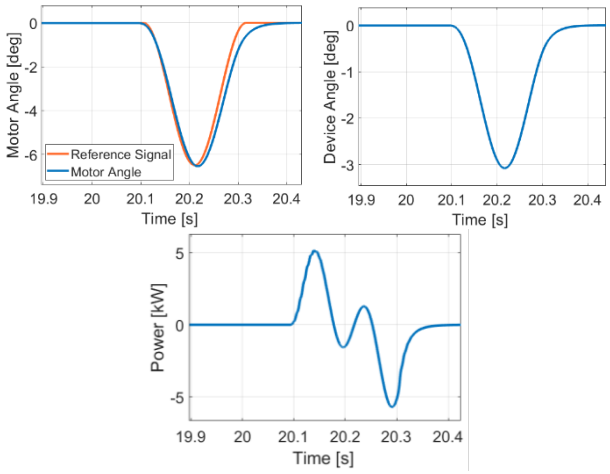

FIGURE 13. Motor angle (top left), device angle (top right) and one motor's power (bottom) for DN 1 actuated by FBL with RotEMA

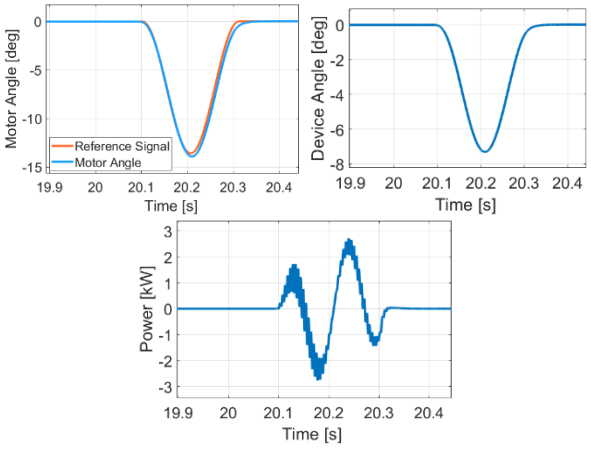

FIGURE 14. Motor angle (top left), device angle (top right) and one motor's power (bottom) for tab 1 actuated by FBL with RotEMA

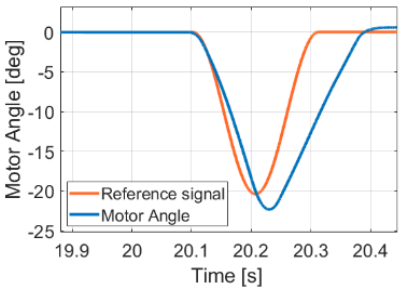

FIGURE 15. Motor angle for tab 1 actuated by FBL with RotEMA for 150% actuation rate

6. EVALUATION ON OVERALL SYSTEM LEVEL

Regarding the overall power required for load control, the generated results are assumed to be sufficiently accurate. Further aspects, such as power losses due to cable resistance and possible required power for cooling, are neglected in this work. Thus, the total maximum power required for the selected actuation system, consisting of a four-bar linkage with RotEMA, equals 120 kW for both wing sides, as postulated in section 4.2. It should be noted that the maximum stated power demand only occurs for a very limited duration to compensate the critical gust load. The impact of consecutive gust loads on the actuation design is not investigated in this paper. The likelihood of a critical gust occurring is thus also undetermined. To determine the total system weight, cable masses are determined in addition to the masses of the actuation system. The weight of the cable network, depicted in figure 6, is sized according to methods presented in [18], based on maximum current capacity and voltage drop limited to 3%. A conventional AC supply voltage of 230 V is assumed and the signal wiring is not accounted for. Only the cable masses inside the wing are considered, as the electrical architecture inside the fuselage is undefined. For both wing sides, a total cable mass of 124 kg is determined. Regarding generator weight, it is assumed no re-design of the generators is necessary and thus no additional weight is gained. No additional components like AC/DC-converters or transformer rectifier units are accounted for in this paper.

Based on these results, a comparison between the dynamic load control system discussed in this paper and a conventional high-lift system is presented in table 6.

The conventional high-lift system considered consists of flaps and slats, each of which are actuated by a power control unit, positioned central inside the fuselage. It is assumed that only high-lift functions have to be fulfilled by the conventional high-lift system and no function for gust or manoeuvre load reduction exists, which results in significantly lower design actuation speeds and loads. Regarding the mass of the dynamic load control system, actuation of the flaps, used for high-lift, are accounted for with a mass of 200 kg. While the flap-tabs and DN are only used in cruise conditions, the flaps are only actuated during approach and take-off, thus the consumed power for actuation of the flaps is unconsidered in calculating the system power of the dynamic load control system. The values of the system weights and the power consumption of the conventional system and flap actuation are generated using the method presented in [19]. Correspondingly, the system weights and power consumption of the dynamic load control system are generated using the method presented in this work.

As seen in table 6, the system mass increases moderately

compared to the conventional system, while the required power increases more drastically. As discussed in section 4.2, the power generated by the engines should suffice to operate the dynamic load control system during cruise, without the need for resized generators. The presented maximum power is assumed to only be required for a brief moment, but must be applied within a short period of time. Given the magnitude of the required power, this results in a significant impact on the electric power network of the entire aircraft. To compensate these brief high power demands, electric accumulators or capacitors, which are able to provide high power swiftly, have to be considered in future works. In this regard, the probability of critical gust loads occurring has to be considered as well.

	Conv. High-Lift System (Slats + Flaps)	Dynamic Load Control System (DN + Flaps + Tabs)
System mass [kg]	400	586
Mass-Delta to conv. system [%]	-	147
System power [kW]	30	120
Power-Delta to conv. system [%]	-	400

TAB 6. Comparison of dynamic load control system to conventional high-lift system

6.1. Estimation of potential mass reduction

In [20] the impact of manoeuvre load alleviation (MLA) and gust load alleviation (GLA) methods for the structural design of different reference aircrafts is investigated. One of these reference aircrafts is the D150 configuration, which is similar to the Airbus A320. According to [20], manoeuvre loads evoke the largest wing bending moment for the considered reference aircraft. Furthermore, the wing bending moment influences sizing of the wing structural mass significantly [20]. In [20] a wing root bending moment reduction of only 6.2% results in a wing box mass reduction of 130.5 kg. According to [4], MLA utilized on the LEISA configuration results in a reduction of the wing root bending moment of 33%. The required actuation performance required to achieve the MLA, which is postulated in [4], can still be achieved with the reduced actuation speed for GLA given in section 4.2 of this paper. Additionally, compared to the D150 configuration a higher wing box mass can be assumed for the LEISA configuration, due to higher wingspan and wing area. Thus, due to higher reduction of the wing root bending moment and higher wing box mass, it is assumed that a wing box mass reduction of over 1000 kg can be achieved. However, the additional weight of the dynamic load control system of 186 kg, compared to a conventional high-lift system, has to be considered. Accounting for this additional system weight, a total aircraft mass reduction of roughly around 1000 kg can be assumed. Admittedly, the estimation method used in this section presents a crude way of predicting structural mass reduction through dynamic load control, but presents a rough estimate of the potential of dynamic load control systems regarding mass reduction and consequentially decrease of fuel demand. Nonetheless, the potential for high reduction of total aircraft mass by utilizing dynamic load control is evident.

7. CONCLUSION

In the present paper, a design method and results of actuation systems for fast actuated droop noses and flap-tabs used for dynamic load control were presented and discussed. Dynamic load control enables the reduction of the wing structural mass by reducing critical loads occurring during gust scenarios. The reference aircraft and the critical load cases were presented, which indicated ambitious actuation speeds and loads, required to considerably reduce forces acting on the structure. A variety of actuation concepts were considered to fulfil the stated requirements and a reliability analysis was carried out. The method used for a preliminary investigation, based on a genetic optimization algorithm, was presented and a preliminary sizing of the introduced concepts was performed to evaluate the optimal system for actuation of the DN and flap-tabs. Based on these investigations, a RotEMA in combination with a FBL was selected for further investigation. It could be shown that the fulfilment of the previously established requirements was not feasible on a system level, since the required power far exceeds conventionally available power. With increased available power for the actuation system and more efficient actuator concepts the established requirements might be fulfilled. However, in this work reduced requirements were investigated by individually lowering the actuation speed demands of the corresponding control devices, resulting in a feasible actuation concept proposition, considering conventionally available power, which was further investigated. To verify the preliminary design results, performance analyses were conducted using simulation models. The preliminary determined power demands were demonstrated to correspond well with the simulation results and the possibility of oversizing was dismissed. Lastly, the impact of a dynamic load control system on the overall system level was investigated and the dynamic load control system was compared to a conventional high-lift system. This comparison resulted in a moderate increase of system mass, but a significant rise of system power. An estimation of potential total aircraft mass reduction was carried out, which indicated severe mass reductions can be achieved by introducing a dynamic load control system.
This work focused on the preliminary analysis and showed the potential of the innovative dynamic load control concept. Additional aspects, like cooling of the actuation systems, the impact of high power consumption for a very short duration on the overall electric system, the possibility of consecutive impact of gust loads and the potential overall aircraft mass reduction were neglected or only briefly touched upon in this work. The impact of structural mass was roughly approximated in this paper. In future works the estimation of the potential reduction of structural mass needs to be considered in more detail. Furthermore, demonstrators can be used to validate the results of this work, account for additional aspects, like cooling or fault scenarios, and analyse real behaviour.

©2024

ACKNOWLEDGEMENT

The results of the presented paper are part of the work in the research project Overall Concepts for Actuation Systems of Dynamic Control Surfaces for the Reduction of Loads on an Intelligent Wing (INTELWI), which is supported by the Federal Ministry of Economic Affairs and Climate Action in the national LuFo VI program. Funding code for TUHH: 20A1903K, for USTUTT: 20A1903B and for TUBS: 20A1903J. Any opinions, findings and conclusions expressed in this document are those of the authors and do not necessarily reflect the views of the other project partners.

Supported by:

Federal Ministry
for Economic Affairs
and Climate Action

on the basis of a decision
by the German Bundestag

BIBLIOGRAPHY

[1] Ullah, Junaid, et al. "Approach for Aerodynamic Gust Load Alleviation by Means of Spanwise-Segmented Flaps." Journal of Aircraft 60.3. 2023

[2] Dargel, G., et al. „Aerodynamische Flügelauslegung mit multifunktionalen Steuerflächen," DGLR, Bonn [Hrsg.]: DGLR Jahrbuch 2002

[3] Wild, Jochen, Michael Pott-Pollenske, and Björn Nagel. "An integrated design approach for low noise exposing high-lift devices." *3rd AIAA Flow Control Conference*. 2006.

[4] Breitenstein, Christian, et al. "Fluid-Structure Coupled Analysis of Maneuver Load Alleviation on a Large Transport Aircraft." AIAA AVIATION 2023 Forum. 2023.

[5] European Aviation Safety Agency: Certification Specifications and Acceptable Means of Compliance for Large Aeroplanes: CS-25 Amendment 27, 2023

[6] Arriola Gutierrez, David Antonio. Model-based design and fault-tolerant control of an actively redundant electromechanical flight control actuation system. Diss. Technische Universität Hamburg, 2019.

[7] S-18 Aircraft and Sys Dev and Safety Assessment Committee. Guidelines and methods for conducting the safety assessment process on civil airborne systems and equipment. SAE International, 1996.

[8] European Aviation Safety Agency: Design Considerations for Minimizing Hazards Caused by Uncontained Turbine Engine and Auxillary Power Unit Rotor Failures AMC 20-128A. 2021.

[9] Postnikov, S., A. Trofimov, and D. Smagin. "Analysis of the power part architecture for short-medium-range aircraft control system with local hydraulic systems by reliability criterion." IOP Conference Series: Materials Science and Engineering. Vol. 868. No. 1. IOP Publishing, 2020.

[10] Maré, Jean-Charles. Aerospace actuators 1: needs, reliability and hydraulic power solutions. John Wiley & Sons, 2016.

[11] Kulshreshtha, A. Remote actuation control system: aircraft flight control for hydraulic-servo and electric actuation. Recent Advances in Aerospace Actuation Systems and Components, Toulouse, France. 2007.

[12] Deb, Kalyanmoy, et al. A fast and elitist multiobjective genetic algorithm: NSGA-II. IEEE transactions on evolutionary computation, 2002, 6. Jg., Nr. 2, S. 182-197.

[13] Selzam, Bianca. "Genetische Algorithmen." Uni Dortmund. 2003.

[14] Kupfer, Christoph. Maßnahmen zur Erhöhung der Lebens- und Nutzungsdauer von Kugelgewindetrieben unter Kurzhubbelastung in elektro-mechanischen Flugsteuerungsaktuatoren. Technische Universität Hamburg, 2021.

[15] Maré, Jean-Charles. Aerospace Actuators 3: European Commercial Aircraft and Tiltrotor Aircraft. John Wiley & Sons, 2018.

[16] Bozhko, Serhiy, Christopher Ian Hill, and Tao Yang. More-electric aircraft: systems and modeling. Wiley encyclopedia of electrical and electronics engineering 1999.

[17] Maré, Jean-Charles. Aerospace actuators 2: signal-by-wire and power-by-wire. Vol. 2. John Wiley & Sons, 2017.

[18] Bielsky, T., Jünemann, M., & Thielecke, F. Parametric modeling of the aircraft electrical supply system for overall conceptual systems design. Deutsche Gesellschaft für Luft-und Raumfahrt-Lilienthal-Oberth eV, 2021

[19] Pfennig, Malte. Methodik zum wissensbasierten Entwurf der Antriebssysteme von Hochauftriebs-systemen. Shaker, 2012.

[20] Handojo, Vega. Contribution to load alleviation in aircraft pre-design and its influence on structural mass and fatigue. Diss. Technische Universität Berlin, 2021.

©2024